SIMULATION OF SEMICONDUCTOR DEVICES AND PROCESSES Vol. 4
Edited by W. Fichtner, D. Aemmer - Zurich (Switzerland) September 12-14, 1991 - Hartung-Gorre

Simulation of Transport over Heterojunctions

Matthew Grupen, Karl Hess, and G. Hugh Song[1]
Beckman Institute and Coordinated Science Laboratory
University of Illinois, Urbana, IL, USA

Abstract

The use of thermionic emission theory versus drift-diffusion in two-dimensional finite difference simulations of carrier transport over heterojunctions is discussed. We show the advantages of a two-dimensional mesh which is double-valued with respect to quasi-Fermi levels at heterojunctions. A heterojunction diode is then simulated using both drift-diffusion and thermionic emission at the heterojunction, and the results are compared. Thermionic emission at hetero-interfaces is also used to simulate current confinement by a wide bandgap blocking region in a p-n diode. We find that the use of thermionic emission theory always improves the results and sometimes provides the conditions necessary for convergence.

Heterojunctions are proving to be very important in the design of many classes of semiconductor devices. They are the key to the high performance of transistor structures such as the HEMT and the HBT [1, 2, 3] and have improved the efficiencies of semiconductor solar cells [4]. They have also made possible novel device structures such as the charge injection transistor (CHINT) and the negative resistance field-effect transistor (NERFET) [5, 6]. And it is, of course, the heterojunction that has made the semiconductor laser a practical, coherent light source suitable for commercial applications [7].

Because the use of heterostructures is so pervasive, the accurate simulation of carrier transport in these structures is of vital interest. Most numerical models assume continuous quasi-Fermi levels at the heterojunction interfaces and use drift-diffusion to describe transport throughout the entire device [8, 9, 10, 11, 12, 13], however, it has been shown in one dimension that quasi-Fermi levels need not be continuous at hetero-interfaces [14]. In this paper, the use of thermionic emission and drift-diffusion at heterojunctions is compared, and a new two-dimensional discretization technique is introduced to more efficiently account for heterojunction points in numerical simulations.

1 Treatment of Transport over Heterojunctions

In conventional drift-diffusion models, the assumption of continuous quasi-Fermi levels can be made in two ways. The first way is to avoid determining carrier transport at a heterojunction and instead set the quasi-Fermi levels at points on either side of the junction equal to one another. Drift-diffusion theory can be used between points away from the heterojunction, and current continuity can be maintained [14]. The second way uses drift-diffusion theory to calculate carrier transport over a heterojunction. In drift-diffusion theory, carrier flux densities can be expressed as

$$\mathbf{J}_n = \mu_n n \nabla F_n \tag{1}$$

[1] Currently employed at BellCore, Redbank, NJ.

$$\mathbf{J}_p = \mu_p p \nabla F_p \tag{2}$$

where μ_n and μ_p are the electron and hole mobilities, n and p are the electron and hole densities, and F_n and F_p are the quasi-Fermi levels for electrons and holes, respectively. Because these expressions contain the gradients of the quasi-Fermi levels, they implicitly require the continuity of the quasi-Fermi levels at the heterojunction.

Indeed, the quasi-Fermi levels need not be continuous at a heterojunction. Carriers can be transferred from a wide bandgap material to a narrow bandgap material at a high rate; strong electron-electron and hole-hole interactions exist so that the carriers on either side of a heterojunction maintain different Fermi-like (or Maxwell-Boltzmann-like) distributions. Exact calculations require an ensemble Monte-Carlo method, but a reasonable approximation can be obtained with thermionic emission theory [15].

Wu and Yang have derived a thermionic emission expression for carrier transport between regions of different effective masses [16]. Figure 1 shows a schematic diagram of the conduction band edge at the heterojunction. The electron current density from region 1 to region 2 is given

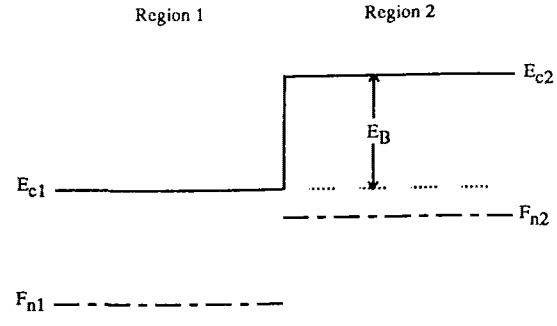

Figure 1: Conduction band edges forming the energy barrier for thermionic emission

by

$$\mathbf{J}_n = \frac{q}{2\pi^2\hbar^3} k^2 T^2 \eta \left[exp\left(\frac{F_{n2} - E_{c2}}{kT}\right) - exp\left(\frac{F_{n1} - E_{c1} - E_B}{kT}\right)\right] \tag{3}$$

where q is the electron charge, $\hbar$ is Planck's constant, k is Boltzmann's constant, and T is the absolute temperature. The coefficient η can account for the different effective masses and the quantum mechanical reflection and transmission at the interface. The simplest expression for η neglects the quantum effects and can be written as

$$\eta = \frac{2}{\frac{1}{m_{n1}} + \frac{1}{m_{n2}}} \tag{4}$$

where m_{n1} and m_{n2} are the effective masses for the free electrons in regions 1 and 2, respectively. An analogous expression exists for holes.

2 Device Model

The basic device equations to be solved are Poisson's equation and the current continuity equations for electrons and holes.

$$-\nabla \cdot \epsilon \nabla \psi + q\left(n - p - N_D^+ + N_A^-\right) = 0 \tag{5}$$

$$\nabla \cdot \mathbf{J}_n + U_{HSR} = 0 \tag{6}$$
$$\nabla \cdot \mathbf{J}_p + U_{HSR} = 0 \tag{7}$$

where ϵ is the static permittivity of the material and ψ is the electrostatic potential. N_D^+ and N_A^- are densities of ionized donors and acceptors, respectively. U_{HSR} is the Hall-Shockley-Reed recombination rate. The free carrier densities are calculated using Fermi-Dirac statistics.

$$n = 2\left(\frac{m_n T}{2\pi\hbar^2}\right)^{\frac{3}{2}} \Im_{\frac{1}{2}}(\eta_n) \tag{8}$$

$$p = 2\left(\frac{m_p T}{2\pi\hbar^2}\right)^{\frac{3}{2}} \Im_{\frac{1}{2}}(\eta_p) \tag{9}$$

$$\eta_n \equiv \frac{F_n - E_c}{kT}, \quad \eta_p \equiv \frac{E_v - F_p}{kT} \tag{10}$$

$$E_c \equiv -q\psi - \chi, \quad E_v \equiv E_c - E_G \tag{11}$$

$$\Im_{\frac{1}{2}}(\eta) = \frac{2}{\sqrt{\pi}} \int_0^\infty \frac{x^{\frac{1}{2}}}{1 + e^{x-\eta}} dx \tag{12}$$

where χ and E_G are the electron affinity and the bandgap, respectively. The ionized impurity concentrations are obtained from the dopant densities.

$$N_D^+ = \frac{N_D}{1 + 2exp\left(\eta_n + \frac{\epsilon_D}{kT}\right)} \tag{13}$$

$$N_A^+ = \frac{N_A}{1 + 4exp\left(\eta_p + \frac{\epsilon_A}{kT}\right)} \tag{14}$$

where $\epsilon_{D(A)}$ is the absolute value of the donor (acceptor) energy level with respect to the conduction (valence) band edge. For the Hall-Shockley-Reed recombination rate, the following expression was used.

$$U_{HSR} = \frac{np - n_i^2}{\tau_n(n + n_1) + \tau_p(p + p_1)} \tag{15}$$

where n_i is the intrinsic carrier concentration, τ_n and τ_p are the carrier lifetimes for electrons and holes, respectively, and n_1 and p_1 are the electron and hole densities when the Fermi level is positioned at the trap energy level. The material parameters for $Al_xGa_{1-x}As$ were obtained from a paper by Adachi [19].

Carrier transport in bulk material is calculated using the drift-diffusion expressions (1) and (2). The carrier current densities at heterojunctions are determined using equation (3).

3 Numerical Method

The device equations have been discretized onto an automatically generated mesh of both rectangles and triangles [17]. The equations are box-discretized using a generalized Scharfetter-Gummel scheme in the bulk regions of the device [20]. Applying this scheme to points around heterojunctions leads to problems when thermionic emission theory is included. Thermionic emission dominates drift-diffusion within a mean free path around the heterojunction. If mesh points are placed this close to a heterojunction, and a quasi-uniform mesh is created away from the junction to minimize truncation error, a prohibitively large number of mesh points may

result. To avoid this problem, mesh points were placed directly at the location of the heterojunction. Any points located at a heterojunction are considered to be double-valued with respect to the quasi-Fermi levels for electrons and holes. In other words, any heterojunction point is treated as two points superimposed on one another when forming the continuity equations. We refer to the additional points as virtual points because they do not exist during the generation of the mesh and yet they are treated explicitly during the discretization of the device equations. This technique is represented schematically in figure 2. Since the expression for thermionic

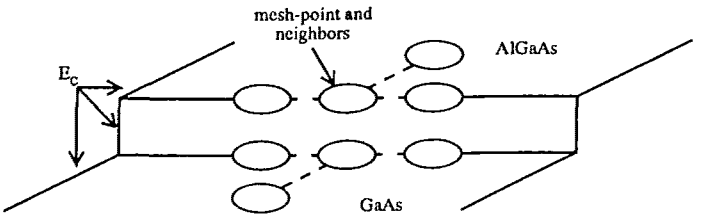

Figure 2: Treatment of mesh points for the continuity equations at a heterojunction

emission contains no spacial gradients and has no truncation error, the virtual points do not add any additional error to the discretized continuity equations. Also, since the heterojunction points are single-valued with respect to electrostatic potential, Poisson's equation is unaware of the superimposed points and the mesh appears to maintain quasi-uniformity.

Simple ohmic contacts have been assumed at electrode boundary points, and Neumann boundary conditions are used for points at free surfaces. The complete set of discretized device equations is solved by the full-Newton method using the Yale Sparse Matrix Package.

4 Calculated Example

The n-$GaAs$/N-$Al_{0.3}Ga_{0.7}As$ diode shown in figure 3 was chosen to illustrate this treatment of transport over a heterojunction. The $GaAs$ region is doped with 1.0×10^{15} cm^{-3} and the

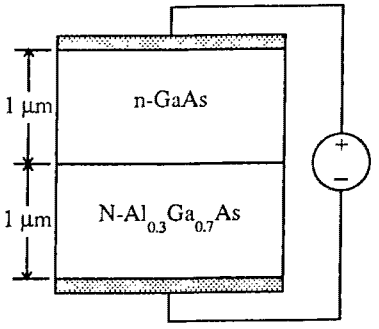

Figure 3: n-N Heterojunction diode: the $GaAs$ and $AlGaAs$ are doped to levels of 1.0×10^{15} cm^{-3} and 1.0×10^{16} cm^{-3}, respectively

$AlGaAs$ region with 1.0×10^{16} cm^{-3} donors. According to the work of Horio and Yanai, in such a structure, the carrier transport across the heterojunction is the rate-limiting process [14].

Consequently, the importance of thermionic emission is most pronounced. Also, such an isotype heterojunction has important device applications such as the current blocking regions in a semiconductor laser.

Figure 4 shows the significant difference between the diode's forward biased I-V characteristics when calculated using drift-diffusion and thermionic emission at the heterojunction. Figures 5 and 6 explain the reason for the differences. Figure 5 shows the band structure for

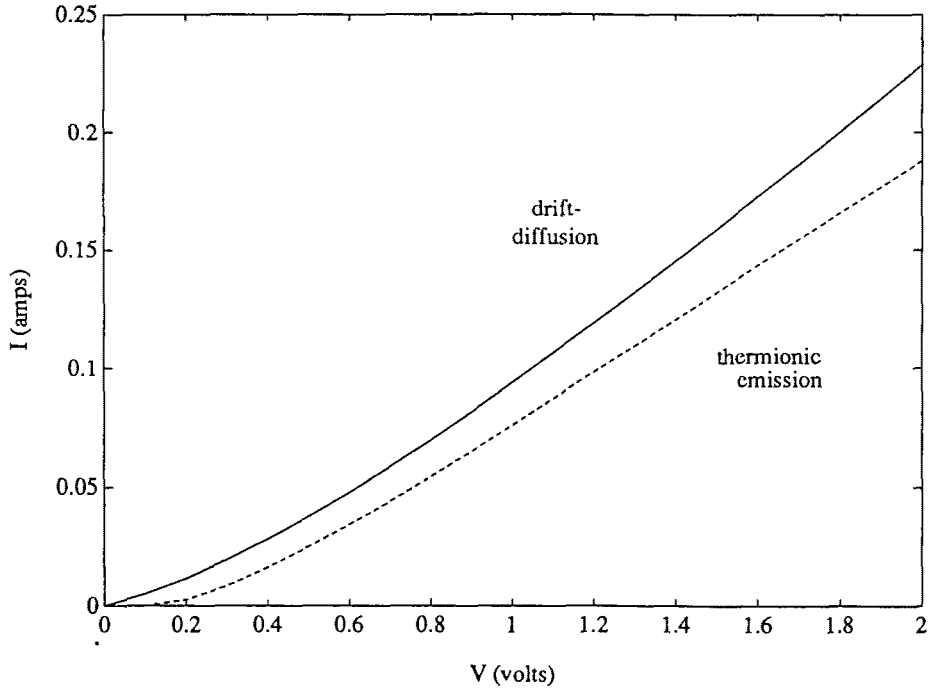

Figure 4: Forward biased I-V characteristics calculated with drift-diffusion and thermionic emission at the heterojunction

the drift-diffusion case. Note the continuous electron quasi-Fermi level at the interface which drift-diffusion theory requires. The band structure for the thermionic emission case, figure 6, shows an abrupt discontinuity in the electron quasi-Fermi level at the interface. This is a more physically accurate description of the device.

Thermionic emission between double-valued mesh-points was also included in a two-dimensional simulation to demonstrate current confinement in a vertical p-n diode. Figure 7 shows the diode structure and the current contour lines within the device with a 2 volt bias. The $GaAs$ p-n diode contains a wide bandgap $Al_{0.5}Ga_{0.5}As$ blocking region at the top electrode. This structure is analogous to what one might find in a semiconductor laser. The transport at the $GaAs/Al_{0.5}Ga_{0.5}As$ interfaces was calculated using thermionic emission. The result is an accurate simulation of the current confinement around the wide bandgap blocking region. Drift diffusion did not lead to convergent results in this case at all and, therefore, cannot be shown for comparison.

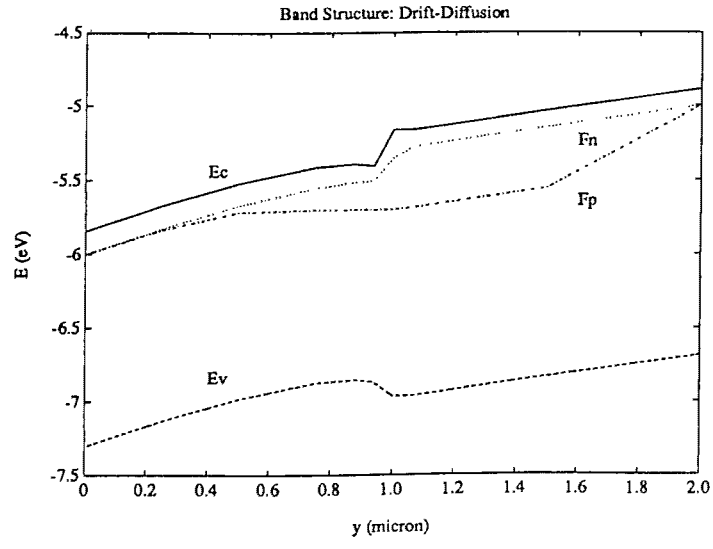

Figure 5: Energy band structure for the n-N diode calculated using drift-diffusion at the heterojunction

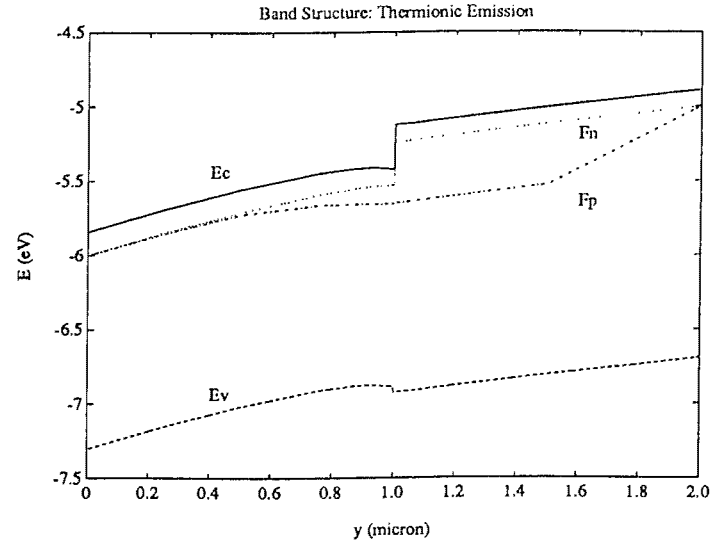

Figure 6: Energy band structure for the n-N diode calculated using thermionic emission at the heterojunction

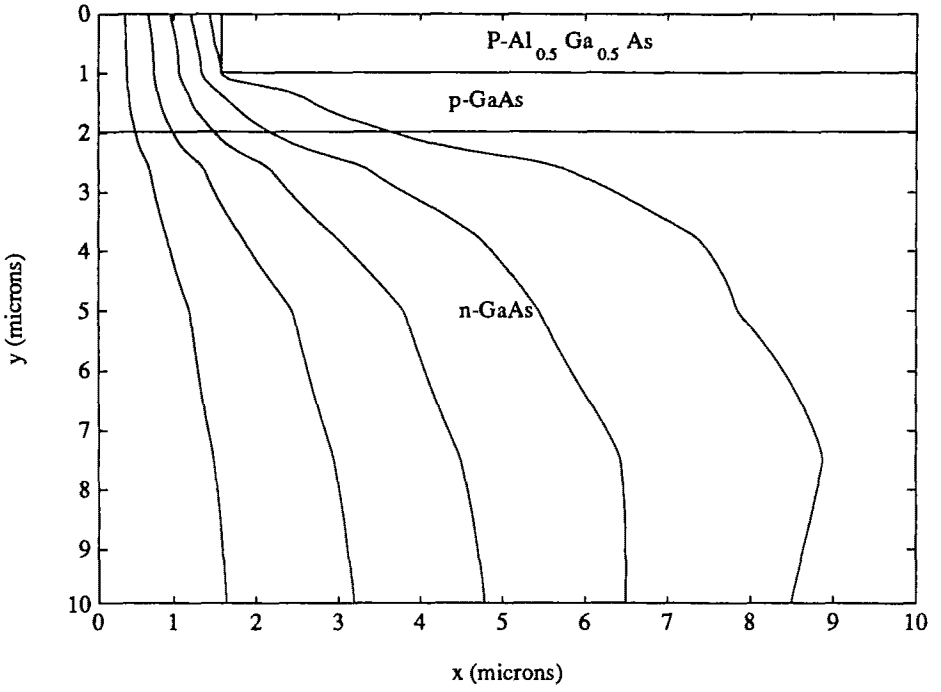

Figure 7: Current confinement around a blocking region calculated with thermionic emission

5 Conclusion

Heterostructures have been studied and modeled extensively. However, the transport of free carriers over heterojunctions typically assumes a continuous quasi-Fermi level. Such an assumption is not realistic. A more accurate treatment of heterojunction transport uses thermionic emission to describe transport between points at a heterojunction. This can be done economically by using mesh points that are double-valued with respect to the quasi-Fermi levels at the heterojunctions. By using such a technique, we have demonstrated the applicability of thermionic emission at heterojunctions in a full two-dimensional simulation.

6 Acknowledgments

Support by the SDIO-IST program through the Office of Naval Research and by NSF through the Illinois Engineering Research Center is gratefully acknowledged.

References

[1] I. C. Kizilyalli, K. Hess, J. L. Larson, and D. J. Widiger, "Scaling properties of high electron mobility transistors," *IEEE Trans. Electron Devices,* Oct. 1986.

[2] J.Y.F. Tang, "Two-dimensional simulation of MODFET and *GaAs* Gate heterojunction FET's," *IEEE Trans. Electron Devices,* Sept. 1985.

[3] M.E. Hafizi, C.R. Crowell, and M.E. Grupen, "The DC characteristics of *GaAs/AlGaAs* heterojunction bipolar transistors with application to device modeling," *IEEE Trans. Electron Devices,* vol. 37, Oct. 1990, pp. 2121–2129.

[4] J.E. Sutherland and J.R. Hauser, "A computer analysis of heterojunction and graded composition solar cells," *IEEE Trans. Electron Devices,* vol. ED-24, April 1977, pp. 363–372.

[5] A. Kastalsky and S. Luryi, "Novel real-space hot-electron transfer devices," *IEEE Electron Device Lett.,* vol. EDL-4, Sept. 1983, pp. 334–336.

[6] I.C. Kizilyalli and K. Hess, "Physics of real-space transfer transistors," *J. Appl. Phys.,* vol. 65, March 1989, p. 2005.

[7] G.P. Agrawal and N.K. Dutta, *Long-Wavelength Semiconductor Lasers.* New York: Van Nostrand Reinhold Company, 1986.

[8] K. Yokoyama, M. Tomizawa, and A. Yoshii, "Accurate modeling of *AlGas/GaAs* heterostructure bipolar transistors by two-dimensional computer simulation," *IEEE Trans. Electron Devices,* vol. ED-31, Sept. 1984, pp. 1222–1229.

[9] M. Madihian, K. Honjo, H. Toyoshima, and S. Kumashiro, "The design, fabrication, and characterization of a novel electrode structure self-aligned HBT with a cutoff frequency of 45 GHz," *IEEE Trans. Electron Devices,* vol. ED-32, July 1987, pp. 1817–1823.

[10] J.Y.F. Tang, "Two-dimensional simulation of MODFET and *GaAs* gate heterojunction FET's," *IEEE Trans. Electron Devices,* vol. ED-32, Sept. 1985, pp. 1817–1823.

[11] J.Y.F. Tang and S.E. Laux, "A program to simulate the heterojunction devices in two dimensions," *IEEE Trans. Electron Devices,* vol. CAD-5, Oct. 1986, pp. 645–652.

[12] M.S. Lundstrom and R.J. Schuelke, "Numerical analysis of heterostructure semiconductor devices," *IEEE Trans. Electron Devices,* vol. ED-30, Sept. 1983, pp. 1151–1159.

[13] T. Ohtoshi et. al., "A two-dimensional device simulator of semiconductor lasers," *Solid-State Electron.,* vol. 30, 1987, pp. 627–638.

[14] K. Horio and H. Yanai, "Numerical modeling of heterojunctions including the thermionic emission mechanism at the heterojunction interface," *IEEE Trans. Electron Devices,* vol. ED-37, April 1990, pp. 1093–1098.

[15] K. Hess, *Advanced Theory of Semiconductor Devices.* Englewood Cliffs: Prentice Hall, 1988.

[16] C.M. Wu and E.S. Yang, "Carrier transport across heterojunction interfaces," *Solid-State Electron.,* vol. 22, 1979, pp. 241–248.

[17] S. Müller, K. Kells, and W. Fichtner, *Automatic Rectangle-based Adaptive Mesh Generation Without Obtuse Angles.* Swiss Federal Institute of Technolgy, Integrated Systems Laboratory, July 1990.

[18] G.H. Song, K. Hess, T. Kerkhoven, and U. Ravaioli, "Two-dimensional simulation of quantum well lasers," *European Trans. Telecom. Related Tech.*, vol. 1, July–Aug. 1990, pp. 375–381.

[19] S. Adachi, "$GaAs$, $AlAs$, and $Al_xGa_{1-x}As$: material parameters for use in research and device applications," *J. Appl. Phys.*, vol. 53, 1985, pp. 67–77.

[20] D.L Scharfetter and H.K. Gummel, "Large scale analysis of a silicon Read diode oscillator," *IEEE Trans. Electron Devices*, vol. ED-16, 1969, pp. 67–77.